

Revealing AGN, young and old stellar populations in HzRGs with PEGASE.3

Guillaume Drouart^{1,2,3}, Carlos De Breuck¹, Joël Vernet¹,
Brigitte Rocca Volmerange² and Nicholas Seymour³

¹ESO, Karl Schwarzschild Straße 2, 85748 Garching bei München, Germany

²Institut d'Astrophysique de Paris, 98bis boulevard Arago, 75014 Paris, France

³CSIRO Astronomy & Space Science, PO Box 76, Epping, NSW 1710, Australia
email: drouart@iap.fr

Abstract. The HeRGÉ (*Herschel* Radio Galaxy Evolution) project consists of a sample of 70 radio galaxies in the range $1 < z < 5.2$. They benefit from continuous coverage from 3 to $870\ \mu\text{m}$ with *Spitzer*, *Herschel* and sub-mm ground-based instruments (SCUBA, LABOCA). As a calorimeter, IR is an excellent proxy to estimate the contribution of both AGN and starburst, making of radio galaxies perfect candidates to provide new insights into the relationship between AGN and their host galaxies. The IR SED fitting with empirical templates reveals that radio galaxies are luminous and that their black holes and their host galaxies are not growing simultaneously. Extending the SED to optical/near-IR on a subsample of 12 radio galaxies spanning $1 < z < 4$ reveal the necessity of three components to reproduce the observations. Making use of the evolutionary code PEGASE.3 and an AGN torus model, we are able to estimate parameters from the AGN torus, the evolved stellar population and the starburst (SB). They reveal that radio galaxies are massive, evolved, forming the bulk of their mass at very high redshift in a short timescale, but experience episodic, strong SB events, often associated with an AGN activity.

Keywords. Galaxies: high redshift, active, evolution, stellar content – Infrared: galaxies

Powerful radio galaxies (HzRGs) are detected out to $z = 5$. These particular galaxies have many interesting properties to understand the formation and evolution of galaxies. They are massive ($>10^{11}\ M_{\odot}$), dominated by an evolved stellar population associated with an elliptical galaxy (e.g. Rocca-Volmerange *et al.* 2004, Seymour *et al.* 2007). This suggests that these HzRGs could be the progenitors of the giant elliptical or cluster dominant galaxies observed in the local Universe. HzRGs are also known to exhibit high sub-mm flux densities, suggesting important star formation rates (e.g. Reuland *et al.* 2004). Observations from optical to mid-IR also suggest an important contribution from the AGN (e.g. De Breuck *et al.* 2010, Drouart *et al.* 2012). For the first time, the mid- and far-IR is now observed thanks to the unique coverage offered by *Herschel Space Observatory*. With this complete coverage of the IR SED, it is possible to characterise the AGN and the SB, the two main processes responsible for the dust emission. Indeed, UV/optical light is absorbed by the dust and re-emitted in the IR as thermal emission. The IR emission appears as a footprint of the AGN and young stars intrinsic properties, providing us with a unique opportunity to test the “AGN-SB connection”.

1. Black hole and their host galaxy are not growing simultaneously

Our sample of 70 powerful radio galaxies (HzRGs) have been selected to cover homogeneously the radio luminosity-redshift plane (Seymour *et al.* 2007; $L^{3\ \text{GHz}} > 10^{26}\ \text{WHz}^{-1}$; $1 < z < 5.2$). This sample benefits from *Spitzer* (De Breuck *et al.* 2010) and recently

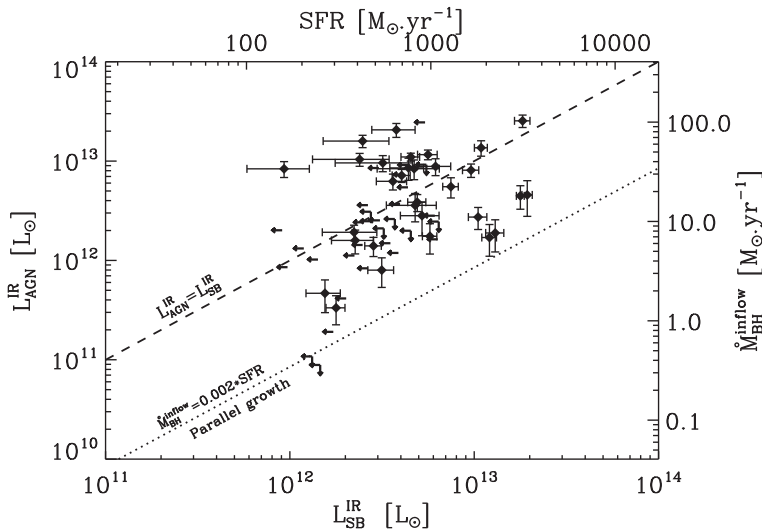


Figure 1. $L_{\text{AGN}}^{\text{IR}}$ versus $L_{\text{SB}}^{\text{IR}}$. The top axis converts $L_{\text{SB}}^{\text{IR}}$ to SFR using the Kennicutt(1998) relation. The right axis converts $L_{\text{AGN}}^{\text{IR}}$ to \dot{M}_{BH} assuming $\epsilon = 0.1$ and $\kappa_{\text{AGN}}^{\text{Bol}} = 6$. The dashed line marks $L_{\text{AGN}}^{\text{IR}} = L_{\text{SB}}^{\text{IR}}$. This dashed line indicates the relation corresponding to $\dot{M}_{\text{BH}} = 0.024 \times \text{SFR}$, using the right and top axis. The dotted line represents the parallel growth mode, where black holes and galaxies are growing simultaneously, following the $\dot{M}_{\text{BH}}\text{-}M_{\text{Gal}}$ relation (see text for details). Figure from Drouart *et al.* 2014.

from *Herschel* (Drouart *et al.* 2014) data covering for the first time the entire IR SED. HzRGs appear to be luminous in the IR ($L_{\text{tot}}^{\text{IR}} > 10^{12} M_{\odot}$) but indistinguishable from standard ULIRGs. We made use of the fitting code DecomPIR to disentangle between the AGN and the SB components in order to explore the “AGN-SB connection”. Our sample spans the entire spectrum of AGN and SB relative contribution, from SED AGN- to SB-dominated, with most of the sources in an intermediate regime. In the case of HzRGs, no clear correlation is found between AGN and star forming activity (Fig. 1). This results is both in agreement (e.g. Feltre *et al.* 2013) and in disagreement (e.g. Netzer *et al.* 2009) with previous studies, the origin of this difference is still hard to quantify.

As most of the energy is emitted in the IR, assuming simple physical assumptions, it is possible to estimate the star formation rate (SFR) and the black hole accretion rate (\dot{M}_{BH}). The SFR is calculated using the canonical law from Kennicutt 1998, while \dot{M}_{BH} is calculated using $\kappa_{\text{AGN}}^{\text{Bol}} \times L_{\text{AGN}}^{\text{IR}} = \epsilon \dot{M}_{\text{BH}} c^2$, where $\kappa_{\text{AGN}}^{\text{Bol}}$ is the bolometric correction factor to convert $L_{\text{AGN}}^{\text{IR}}$ to $L_{\text{AGN}}^{\text{Bol}}$. $L_{\text{AGN}}^{\text{IR}}$ is the integrated AGN luminosity in the 8–1000 μm in L_{\odot} , ϵ the radiative efficiency, c the speed of light and \dot{M}_{BH} , the accretion rate in $M_{\odot}\text{yr}^{-1}$. Our calculated SFR and \dot{M}_{BH} are reported on the opposite axis (top and right) in Fig. 1 (we assume $\epsilon = 0.1$ and $\kappa_{\text{AGN}}^{\text{Bol}} = 6$ for the conversion into \dot{M}_{BH}).

HzRGs in our sample span a wide range in both SFR and \dot{M}_{BH} , 100–5000 $M_{\odot}\text{yr}^{-1}$ and 1–100 $M_{\odot}\text{yr}^{-1}$, respectively. How black holes are growing relatively to their host galaxies? Assuming HzRGs will reach the observed local $\dot{M}_{\text{BH}}\text{-}M_{\text{Gal}}$ relation ($\dot{M}_{\text{BH}} \approx 0.002 M_{\text{Gal}}$) and taking the assumption of a parallel growth, one can calculate the expected function for black hole and galaxy growth (dotted line in Fig. 1). We remark that HzRGs are not following this regime and even present an offset of about one order-of-magnitude above this line. This result has one immediate implication: the black hole and its host galaxy in the HzRGs are not growing in lock step. The HzRGs are therefore experiencing an important growth of their black holes and their host galaxies, but relatively speaking, a

more important black hole growth. This makes of HzRGs very similar to high- z quasars, with large \dot{M}_{BH} . The observed AGN luminosity in the IR are not directly related to the radio emission but more to an intense radiative phase similar to quasars. We stress here that this results is mass independent (both on stellar and black hole masses), the only assumptions are the local $M_{\text{BH}}\text{-}M_{\text{Gal}}$ relation and a parallel growth.

Several uncertainties deserve a discussion. First, AGN activity varies over time relatively quickly. Nevertheless, this variation can induce scatter in our relation, but will not change the average over our sample. Second, the bolometric correction can be uncertain. Indeed, we set here $\kappa_{\text{AGN}}^{\text{Bol}} = 6$. However, even taking $\kappa_{\text{AGN}}^{\text{Bol}} = 2$, the observed offset in Fig. 1 will still be significant though the \dot{M}_{BH} should be lowered by a factor of 3. Third, the radiative efficiency set here to $\epsilon = 0.1$. Several studies suggest a variation from $\epsilon = 0.06$ to $\epsilon = 0.4$. Again, changing ϵ will not affect the general offset of our sample. Finally, the *Herschel* data suffer of a poor resolution (~ 20 arcsec). The estimated SFR could therefore be contaminated by nearby companions (e.g. Ivison *et al.* 2012). Even if this effect can be of a factor of a few, this will not affect our general conclusion.

2. Early formed galaxies with episodic activity (AGN and SB)

On the previously introduced sample, we focus on the sources with the highest data quality. By high quality, we mean sources with *Herschel* detections in most bands and optical, near-IR data available. We therefore create a subsample of 12 radio galaxies spanning $1 < z < 4$. We use this large number of broad band photometries conjointly with two codes, PEGASE.3 (Fioc *et al.*, in prep) and an AGN torus model (Fritz *et al.*, 2006), in order to better disentangle the AGN, the young and the old stellar populations. PEGASE.3 calculates the emission at any age of a stellar population for a given scenario (IMF, star formation law, infall, galactic winds), predicting consistently the dust emission from the metal enrichment of the interstellar medium (ISM) through stellar evolution (SN, TP-AGB). The AGN torus model predicts the AGN emission for a central point source and various torus properties (size, dust density profiles, opening angle, inclination). One important property is that the two codes predict the emission from UV to far-IR.

Previous studies showed that the near-IR emission is dominated by stellar emission, most likely from an evolved stellar population (e.g. Rocca-Volmerange *et al.* 2004; Seymour *et al.* 2007). On one hand, important flux densities suggest a vigorous star formation (e.g. Reuland *et al.* 2004). On the other hand, the mid-IR is also clearly dominated by an AGN contribution (e.g. De Breuck *et al.* 2010; Drouart *et al.* 2012). We use various combinations of a an evolved stellar component, associated with a hybrid template consisting of the sum of an AGN and a SB template. While one or two components are not able to reproduce the entire SED, three components (one AGN and two stellar populations) can satisfactorily reproduce our observed UV–far-IR SED.

The results from our SED fitting provide us with quantity of information on the AGN and its host galaxy. The necessity of two stellar components is clear, and confirm our previous results (Rocca-Volmerange *et al.* 2013). Fig. 2 presents the results on the age and the mass of the 12 radio galaxies. An evolved ($> 1\text{Gyr}$) and massive ($> 10^{11} M_{\odot}$) dominates the near-IR emission. Already in place at $z \sim 4$, the scenario needed to reproduce such a population implies a rapid collapse of an important mass of gas at very high redshift. This scenario also corresponds to the scenario to reproduce elliptical or S0 galaxies in the local Universe. A young stellar population, dense ($K = 10$), young ($< 100\text{Myr}$) and massive ($> 3 \times 10^{10} M_{\odot}$) is also required to reproduce the SED. This SB is supposed here to be short ($< 1\text{Myr}$) with a null initial metallicity ($Z = 0$). The density required to reproduce the far-IR SED is ten times larger than the N_{HI} in the Milky Way. The AGN

component appears to be highly variable from source to source and do not correlate with stellar population properties. We will investigate further the effect of the initial metallicity, the duration of the SB and the IMF in the near future, but they are expected to only have a minor impact on the calculated masses, thought more important on the ages.

These results imply that HzRG are formed rapidly, during the first hundreds of millions years of the Universe. As suggested previously, HzRGs appear as the progenitors of the massive ellipticals observed in the local Universe. Even if the bulk of their stars have already been formed, they experience massive star formation episodes. The cause of this star formation event is still unclear, due to the poor resolution of far-IR data. HzRGs been often part of disturbed systems, mergers appear as a solution (e.g. Ivison *et al.* 2012), or in denser environments (e.g. Wylezalek *et al.* 2013). Nonetheless, important quantities of molecular gas are possibly aligned with the radio jets, which could trigger star formation (e.g. Bicknell *et al.* 2000, Emonts *et al.* 2013). Only ALMA can reach the resolution and sensitivity required to settle definitively this question.

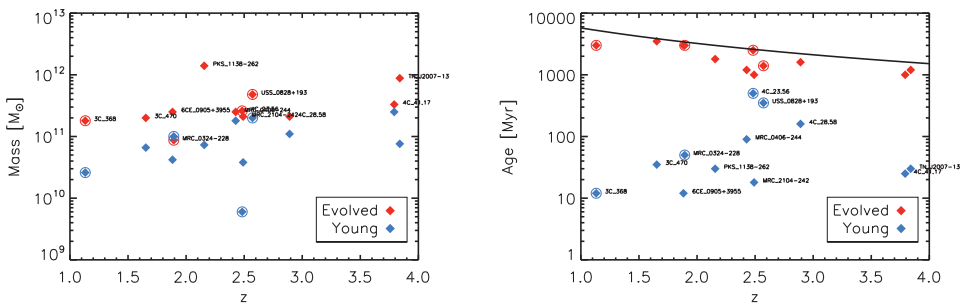


Figure 2. Circles represent less secure fitting solutions. *Left* : mass versus redshift. *Right* : Age versus redshift. The black line represents the age of the Universe at the given redshift assuming the concordance cosmological model ($H_0 = 70 \text{ km s}^{-1} \text{ Mpc}^{-1}$, $\Omega_\Lambda = 0.7$, $\Omega_M = 0.3$). Figure from Drouart *et al.*, in prep.

References

- De Breuck, C., Seymour, N., Stern, D., *et al.* 2010, *ApJ*, 725, 36
Drouart, G., De Breuck, C., Vernet, J., *et al.* 2012, *A&A*, 548, A45
Drouart, G., De Breuck, C., Vernet, J., Seymour, N., *et al.* 2014, *A&A*, 2014arXiv1404.1080D
Emonts, B. H. C., Feain, I., Röttgering, H. J. A., *et al.* 2013, *MNRAS*, 430, 3465
Feltre, A., Hatziminaoglou, E., Hernán-Caballero, A., *et al.* 2013, *MNRAS*, 434, 2426
Fioc, M., Rocca-Volmerange, B., Dwek, E., in prep
Fritz, J., Franceschini, A., & Hatziminaoglou, E. 2006, *MNRAS*, 366, 767
Ivison, R. J., Smail, I., Amblard, A., *et al.* 2012, *MNRAS*, 425, 1320
Kennicutt, Jr., R. C. 1998, *ARA & A*, 36, 189
Netzer, H. 2009, *MNRAS*, 399, 1907
Reuland, M., Röttgering, H., van Breugel, W., & De Breuck, C. 2004, *MNRAS*, 353, 377
Rocca-Volmerange, B., Le Borgne, D., De Breuck, C., Fioc, M., & Moy, E. 2004, *A&A*, 415, 931
Rocca-Volmerange, B., Drouart, G., De Breuck, C., *et al.* 2013, *MNRAS*, 429, 2780
Seymour, N., Stern, D., De Breuck, C., *et al.* 2007, *ApJS*, 171, 353
Wylezalek, D., Galametz, A., Stern, D., *et al.* 2013a, *ApJ*, 769, 79